CrossMark

Integrating geochemical investigations and geospatial assessment to understand the evolutionary process of hydrochemistry and groundwater quality in arid areas

Mohamed El Alfy · Talal Alharbi · Basma Mansour

Abstract Groundwater is the key for life in arid areas. Aquifer overexploitation and climatic conditions can significantly deteriorate groundwater quality. The Al-Qassim area in central Saudi Arabia is characterized by dense agricultural use and is irrigated mainly by fossil groundwater from the Saq Aquifer. Understanding the area's hydrochemistry, major factors governing groundwater quality, and alternative uses of the groundwater are the main goals of this study. Groundwater samples were collected and examined for major, minor, and trace elements. Ionic relationships, hydrochemical facies, geospatial distributions, and multivariate analyses were conducted to assess the hydrochemical processes at play. The salinity and nitrate concentrations of the Saq Aquifer's groundwater were found to increase in the outcrop areas more than the confined areas. The spatial distributions were fragmented by three main factors: (i) modern recharge by relatively brackish water,

(ii) irrigation return flow in intensive farming areas, and (iii) overexploitation and draining of deep and relatively saline zones of the aquifer. Seven water types were found representing the alkaline water with a predominance of sulfate–chloride ions and earth alkaline water with a predominance of sulfate and chloride. Mixing between fresh and brackish water, dissolution of mineral phases, silicate weathering, and reverse ion exchange were recognized as the evolutionary processes, while evaporation played a minor role. Cluster analyses characterized the fresh groundwater zone, modern groundwater recharge zone, and anthropogenic influence zone. In the confined areas, nearly all the groundwater was appropriate for domestic use and irrigation. In the outcrop areas, some limitations were found due to unsuitable conditions.

M. El Alfy
PSIPW Chair, Prince Sultan Institute for Environmental, Water and Desert Research, King Saud University, Riyadh, Saudi Arabia

M. El Alfy (✉)
Geology Department, Faculty of Science, Mansoura University, Mansoura, Egypt
e-mail: melalfy@ksu.edu.sa

T. Alharbi
Geology Department, Faculty of Science, King Saud University, Riyadh, Saudi Arabia

B. Mansour
Geology Department, Faculty of Science, Suez Canal University, Ismailia, Egypt

Introduction

Groundwater is a vital resource in arid areas, where surface water is absent or found in small quantities insufficient to sustain growing human needs. Rainfall in such arid areas is rare, and the temporal and spatial variations are high. The geogenic factors affecting natural groundwater geochemistry are the dissolution and precipitation of various minerals and ion and reverse ion exchange processes (Merkel and Planer-Friedrich 2008; Rasool et al. 2015; Singh and Mukherjee 2015). The

groundwater quality in these arid areas has deteriorated significantly as a result of aquifer overexploitation, land-use/land-cover change, irrigation return flow, unrestricted use of fertilizers and pesticides on farming lands, and incorrect wastewater disposal (Lockhart et al. 2013; Lavoie et al. 2015; El Alfy and Faraj 2017; El Alfy et al. 2017).

The current annual total water consumption in Saudi Arabia is nearly 17.5 billion cubic meters (BCM). Only 5.4 BCM of the consumption is from renewable surface and groundwater, while the annual depletion of fossil groundwater is nearly 12 BCM (World Bank 2012; MoWE, unpublished report, 2014). Agricultural activities are the cornerstone of the Al-Qassim area economy and these activities consume more than 85% of the water supply which is dependent on the fossil water resource (FAO 2009). Aquifer exploitation has sharply increased, and therefore, the groundwater level of Saq Aquifer has declined severally over the past four decades, thereby exacerbating water stress. Additionally, groundwater quality has degraded due to both natural and anthropogenic influences. With increases in population and the expansion of the economic activities, water demand will exceed the current water supply, which can lead to catastrophic water shortages (Chaudhuri and Ale 2014; El Alfy and Merkel 2006; Gleeson et al. 2012; El Alfy 2013).

This study aimed to establish an in-depth understanding of the Saq groundwater hydrochemical characteristics, the processes influencing the groundwater quality, and an evaluation of the groundwater source for potentially alternative uses. The study was conducted by investigating the hydrochemistry of the major, minor, and trace elements, geospatial distribution mapping, and multivariate statistical analyses. Integration of these techniques can help greatly to assess aquifer pollution and address the various natural and anthropogenic factors affecting the groundwater chemistry (Salman et al. 2014; Parizi and Samani 2013; Gemail et al. 2017). The hydrogeology of Saq Aquifer and groundwater quality evaluations have been studied regionally by several researchers (Burdon 1982; Jado and Zotl 1984; Lloyd and Pim 1990; Zaidi and Mukhopadhyay, 2015; Ahmed et al. 2015), and due to the great importance of the aquifer as the main water supply, and its changeable dynamic status, more investigations are needed.

Study area

The Al-Qassim area is an important agricultural center in the central part of Saudi Arabia between 25° 52′–26° 23′ N and 43° 24′–44° 7′ E (Fig. 1) (Al-Bassam 2006). The area is directly east of the Arabian Shield; however, ground elevations range from 600 to 750 m above the mean sea level, and the ground surface slopes slightly to the east. The study area has a typical continental desert climate where the average temperature values vary greatly between day and night, and during the summer and winter months (Almazroui 2011). The mean annual precipitation rate in the Al-Qassim area is < 150 mm, and evaporation rates can reach as high as 3 cm/year leading to a climate with practically very low recharge rates (5–12 mm/year).

Geological and hydrogeological setting

The area of study is located on the Arabian Shelf directly east of the Arabian Shield. The shield area is comprised of Precambrian–Cambrian highlands of igneous and metamorphic rocks, while the shelf consists of an unconformable sedimentary sequence overlying the shield rocks. The shelf rocks dip slightly to the east (1–2°) and become progressively younger (Fig. 1). The area of study is covered by Paleozoic and early Mesozoic sedimentary rocks, which are composed of sandstone, limestone, shale, and gypsum (Powers et al. 1966). The Saq Formation exposed in the form of a belt, parallel to the Arabian Shield, unconformably overlays the basement complex rocks. The Saq rocks consist of white, brown, and red sandstones, which are coarse to fine-grained and poorly cemented. The Saq lithology is homogeneously dominated mainly by sandstones with some minor interbedded shale and siltstone layers. The thickness of Saq Aquifer within the study area ranges from between 350 to 750 m. The area of the study has a multilayered aquifer system whereby the Cambro-Ordovician age Saq sandstone aquifer is considered as the main water resource in Saudi Arabia. The Saq groundwater is easily reachable and economically feasible to the local farmers. The Tabuk, Khuff, and Neogene secondary aquifers also exist and these aquifers are separated from the Saq by the Hanadir, Ra'an, and Qusaiba impervious shales. The well depths tapping Saq Aquifer are below 100 m in the western part in the outcrop area (unconfined), while wells can reach depths exceeding 1200 m in the eastern part where confined conditions prevail.
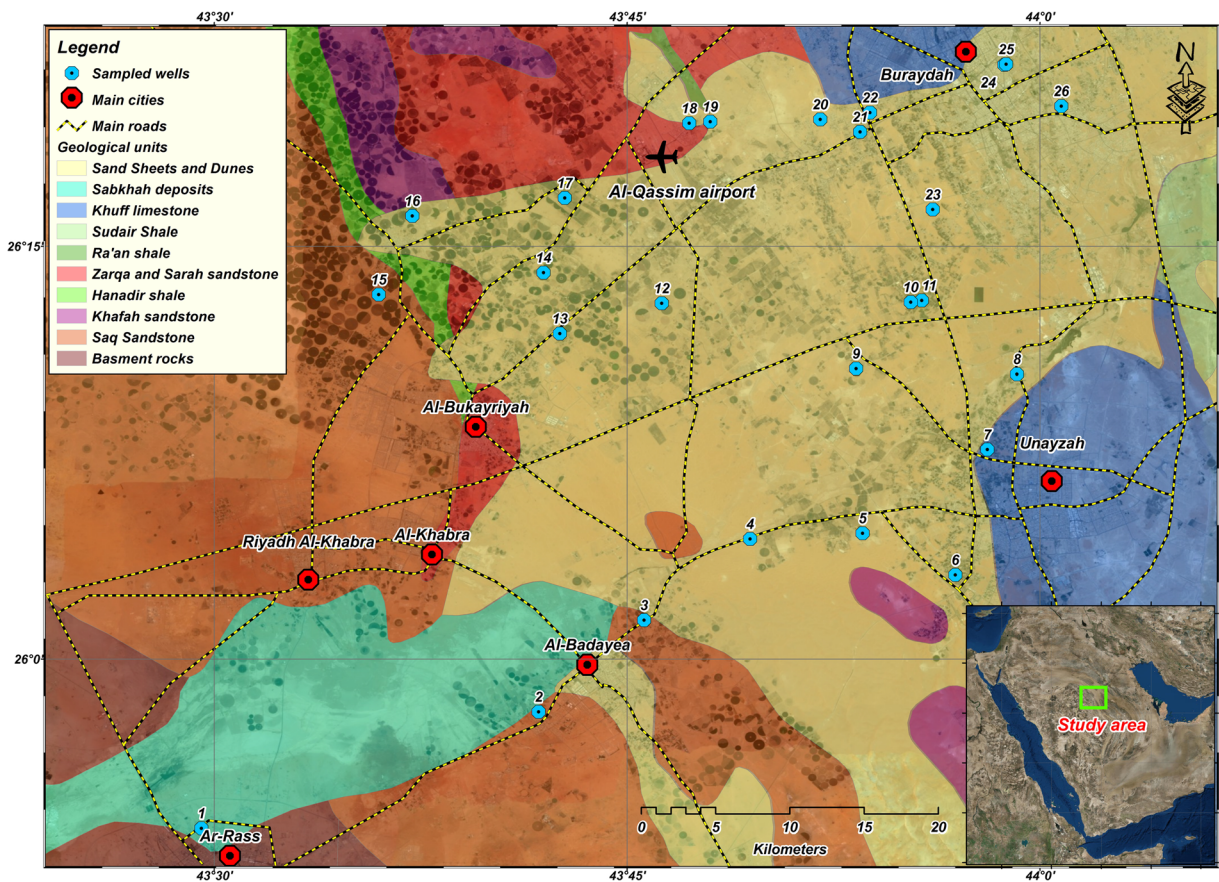
Fig. 1 Location map of the study area, groundwater samples, and geological units

In these areas, near Ash-Shimasiyah and Tanumah, Saq Aquifer is overlain by the Hanadir shale and other younger sedimentary rocks. The depths to water levels vary between 50 m in the western part and 200 m in the eastern part of the aquifer system. The hydraulic parameters of Saq Aquifer are good. Although the pore spaces are partially cemented, good effective porosity (12–20%) is retained. The transmissivity values range between 9×10^{-3} and 4×10^{-2} m^2/s, and the storativity in the unconfined zone from 1.2×10^{-3} to 7×10^{-2}, while the storage coefficients vary from 10^{-4} to 5×10^{-3} in the confined zone. Due to intensive pumping during the last four decades, a huge depression cone has developed in the Buraydah–Unayza area. The water levels dropped between 1960 and 2008 by > 150 m in Buraydah, and > 100 m in the Unayza area in the confined part, and 3–30 m in the outcrop area in the west (Fig. 2).

The current groundwater recharge rate is very limited (3.5–12 mm/year) because of the prevailing arid

climatic conditions. Saq Aquifer recharged during the humid conditions that prevailed in the Middle East during Pleistocene; however, the age of groundwater is 10,000 to 30,000 years (BRGM 1985, 2006).

Land-use pattern and urbanization

Within the study area, different types of land use have been identified. Several dense urbanized areas exist; Ar-Rass City is located at the outlet of Wadi Al-Rummah in the southwestern part of the area; closely downstream to the east are the cities of Al-Badayea, Al-Khabra, and Riyadh Al-Khabra, and in the eastern part the Al-Bukayriyah, Buraydah, and Unayzah cities are found. In the northwestern part, intensive agricultural areas exist where the local inhabitants can easily access the shallow good-quality groundwater. Other smaller farm lands are found near the urbanized areas where lower quality groundwater at relatively greater depths can be found. At the outlet of the Wadi Al-Rummah, there is
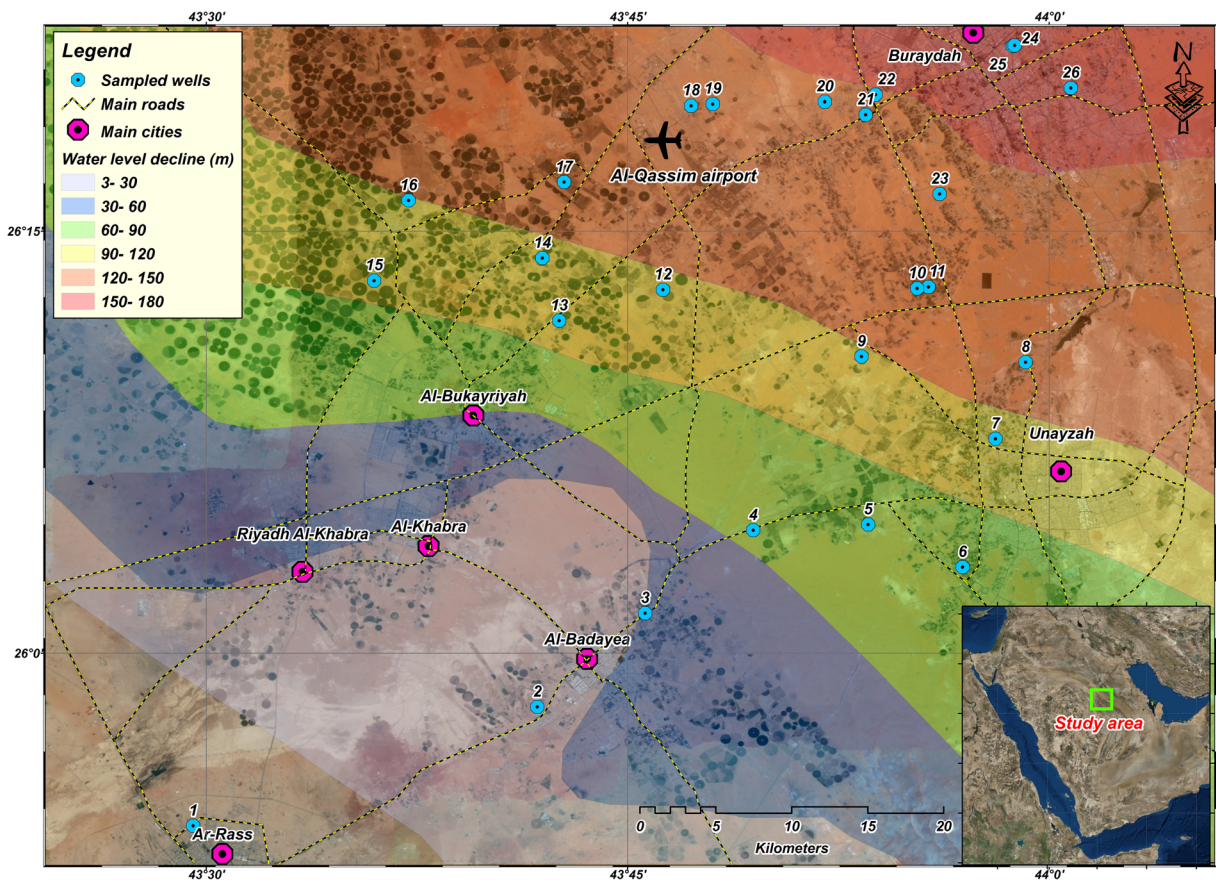
Fig. 2 Water level decline of Saq Aquifer, Badayea area (MoWE, unpublished report, 2008)

a large depression, where a sabkha area has formed; however, runoff water has accumulated there and is subjected to intensive evaporation. The evaporites of the sabkha are leached by the runoff water and percolate to recharge the shallow groundwater with brackish water.

Material and methods

To achieve the study objectives, integrated techniques and approaches have been applied, namely, hydrogeological, hydrochemical, water quality investigations, and geospatial and multivariate statistical analyses. In total, 26 water samples were collected from irrigation and domestic wells tapping Saq Aquifer in December 2015 (Fig. 1). The samples were collected in 1-L polyethylene bottles which were completely filled to avoid degassing prior to chemical analyses. For minor and trace elements,

acidified 100-mL aliquots of filtered (45 μm) groundwater were collected in pre-cleaned low-density polyethylene bottles. Standard methods were used for sample collection, storing, preservation, and analyses (APHA 1995). Several physico-chemical parameters are measured directly in the field, such as the pH, total dissolved solids (TDS), and electrical conductivity (EC), using portable multielectrodes (Hanna Instruments, MI, USA). The major cations (Na^+, K^+, Mg^{2+}, and Ca^{2+}) were analyzed by atomic absorption spectrophotometry (AAS). Bicarbonate (HCO_3^-) and chloride (Cl^-) were examined by titration method. The sulfate (SO_4^{2-}) concentration was estimated using colorimetric methods. Silicon dioxide (SiO_2) was calorimetrically examined by the ammonium molybdate method. Nitrate (NO_3^-) was measured by ion chromatography (ELAN9000). For the trace metals (B^{3+}, F^-, $Fe_{(tot)}$, Mn^{2+}, Pb^{2+}, and Zn^{2+}), inductively coupled plasma–atomic emission spectrometry

(ICP–AES) (Dionex ICS-5000) was used. Ground-water hydrochemistry was studied using the occurrence, relations, and spatial distributions of the major, minor, and trace elements, where several hydrochemical processes were examined to understand the rock–water interactions.

Descriptive statistics, normality tests, and multivariate analyses of the different variables were carried out using the STATISTICA-10 computer package. The spatial distributions of several variables were performed with ArcGIS 10.4 using fitted semi-variogram models, where universal kriging was used to approximate values in unmeasured sites and cross-validations were done to reduce the root mean square error (RMSE). Universal kriging is more truthful than other methods, and the technique was engaged with an accuracy of 3.6 and 3.2 for the distributions of the TDS and NO_3^-, respectively. The semi-variograms were estimated as follows:

$$\gamma(h) = \frac{1}{2n(h)} \sum_{(i,j):h_{ij}=h} (x_i - x_j)^2 \qquad (1)$$

where $\gamma(h)$ is the semi-variance for distance class h, $n(h)$ is the total number of pairs of values at distance h, and h_{ij} is the distance between locations i and j.

Cluster analysis can provide a better understanding of hydrochemical systems through discretization of different groundwater categories which can be significant for a geological setting (Kaufman and Rousseuw 1990; El Alfy 2004). R-mode is suitable for different water quality variables, whereas Q-mode is suitable to identify and determine the chemical components of water (Davis 2002; Tabachnick and Fidell 2006). The cluster analysis is used to differentiate homogeneous subgroups of cases in a population and identify a set of groups, which both minimizes the within-group variation and maximizes the between-group variation. The dendrograms indicate the relative magnitude of the proximity coefficients at which the cases were combined. Ward's method is effective to form clusters that are homogenous and geochemically different from other clusters (Cloutier et al. 2008; El Alfy et al. 2017). The variances of the different variables are standardized to the matching Z scores to escape false classifications caused by dissimilar orders of level and the variances of the variables. A cluster analysis was performed and the Z-standardized input data matrix of 26 samples and 20 variables of hydrochemical composition are shown in the Q-mode

dendrograms. The Z-score values were considered as follows:

$$Zij = \frac{Xi - \mu i}{\sigma i} \qquad (2)$$

where Xi represents the data for the variable i data, and μi and σi are the mean and the standard deviation of the same variable, respectively.

Factor analysis is a multivariate statistical technique that is developed to inspect the underlying patterns or interactions of multiple variables and to condense information into a smaller set of factors for prediction purposes (Hatcher and Stepanski 1994; Davis 2002; El Alfy et al. 2015). The R-mode factor analysis was carried out using 20 variables and was used to find the associations between the physico-chemical variables and to recognize correlations. The principal factor extraction was reached using varimax criteria (Kaiser 1958), which strengthened the loadings of closely correlated variables in each factor (Furi et al. 2012). The scree plot graphical technique was carried out to choose the number of key components to extract.

Results and discussion

The Saq hydrochemistry

The hydrochemical variables and descriptive statistics of the groundwater samples are presented in Table 1. The results indicated that the groundwater of Saq Aquifer is revealing of fresh, moderate to brackish conditions. In the area of study, the Saq groundwater salinity ranged between 534 and 5664 mg/L, with an average of 2061 mg/L and standard deviation of 1687. Nearly 58% of the water samples surpassed the maximum limits for drinking water proposed by the World Health Organization (WHO) in 2011 (1000 mg/L) (WHO 2011). The K^+ concentration extended between 5 and 42 mg/L, with an average value of 17 mg/L. The concentration of Na^+ ions showed a wide range from 59 to 1816 mg/L, with an average of 537 mg/L. The concentration of Ca^{2+} ions varied between 230 and 1053 mg/L, with an average of 398 mg/L. The concentration of Mg^{2+} ions ranged from 12 to 133 mg/L, with an average of 41 mg/L. The Cl^- concentration ranged from 213 to 3408 mg/L, with an average of 1262 mg/L. The SO_4^{2-} concentration ranged from 112 to 1920 mg/L, with an average of 462 mg/L.

Table 1 Chemical analysis of the major, minor, and trace elements of the groundwater samples

ID	pH	EC (μS/cm)	TDS (mg/L)	Ca^{2+} (mg/L)	K^+ (mg/L)	Mg^{2+} (mg/L)	Na^+ (mg/L)	HCO_3^- (mg/L)	Cl^- (mg/L)	NO_3^- (mg/L)	SO_4^{2-} (mg/L)	SiO_2 (mg/L)	TH (mg/L)	B^{3+} (μg/L)	$Fe_{(tot)}$ (μg/L)	Pb^{2+} (μg/L)	Zn^{2+} (μg/L)	Mn^{2+} (μg/L)	F^- (mg/L)	HPO_4^{2-} (mg/L)
1	7.23	5100	2497	456	40	96	400	183	1349	36	350	39	1534	92	6233	0.18	7.10	2.30	0.94	0.058
2	7.22	11,560	5664	677	21	29	1639	114	3408	47	465	45	1810	170	10,094	0.22	13.80	3.00	0.88	0.068
3	7.30	7740	3795	506	24	27	1816	110	3404	45	408	42	1375	122	7869	0.21	11.70	2.60	0.90	0.066
4	7.29	6000	2941	427	10	133	482	134	639	41	1920	40	1614	88	4566	0.16	6.80	2.30	0.98	0.062
5	7.31	4880	2389	1053	20	21	357	153	1349	40	1402	38	2716	80	3020	0.14	6.30	2.50	0.92	0.061
6	7.37	1985	972	231	10	33	110	162	490	37	118	28	713	56	1710	0.11	4.40	2.40	0.85	0.050
7	7.05	1849	906	246	16	26	64	171	426	28	120	28	721	55	1643	0.10	4.10	2.90	0.93	0.048
8	6.92	3160	1547	476	35	66	238	189	710	35	797	30	1460	74	1852	0.12	5.80	2.80	0.96	0.055
9	6.93	2039	999	234	11	35	112	165	497	33	120	30	728	52	1335	0.10	3.60	2.10	0.91	0.049
10	6.95	10,730	5258	676	21	27	1638	112	3398	42	462	44	1799	164	8494	0.21	12.70	2.30	0.88	0.066
11	6.77	3450	1691	369	17	83	272	128	781	38	606	32	1263	76	2887	0.12	5.90	2.80	0.92	0.058
12	7.35	1089	534	239	5	12	207	159	213	33	612	26	646	42	877	0.08	3.10	2.40	0.95	0.035
13	7.53	2163	1060	236	14	39	115	165	502	36	126	26	750	48	1298	0.10	3.40	2.50	0.86	0.050
14	7.21	2185	1071	237	13	37	114	167	501	36	122	31	744	46	1188	0.09	3.80	2.60	0.93	0.051
15	7.42	1487	729	246	15	26	66	166	420	24	116	30	721	44	1028	0.11	3.20	2.40	0.87	0.042
16	7.50	1912	937	234	12	36	113	162	494	34	119	34	733	48	1322	0.10	3.50	2.30	0.91	0.046
17	7.20	1178	577	230	6	20	59	159	401	21	112	26	657	42	832	0.09	3.30	2.70	0.86	0.036
18	7.16	2488	1220	316	8	59	447	134	639	40	1920	32	1032	59	1745	0.12	4.60	3.10	0.95	0.051
19	6.94	11,180	5480	672	19	25	1630	112	3400	45	462	44	1781	166	9244	0.22	12.90	2.90	0.94	0.066
20	7.07	1251	614	236	14	22	60	162	405	22	114	25	680	43	955	0.09	3.20	2.40	0.91	0.038
21	7.08	5760	2823	460	42	101	406	188	1358	37	355	35	1565	85	2501	0.15	6.40	2.70	0.88	0.061
22	7.13	1489	732	235	14	22	61	166	412	25	117	26	677	48	1225	0.09	3.40	2.80	0.90	0.040
23	7.21	1224	600	242	13	23	62	158	414	22	113	26	699	44	1132	0.09	3.40	2.20	0.84	0.036
24	7.27	1129	553	241	11	25	63	158	412	22	114	25	705	43	908	0.06	3.30	2.00	0.88	0.036
25	6.99	6380	3125	499	21	22	1800	108	3395	42	398	40	1337	90	3012	0.15	6.60	2.80	0.94	0.060
26	6.91	9920	4863	666	17	24	1623	108	3388	44	455	42	1762	155	7846	0.20	10.70	2.40	0.91	0.063
Min	6.77	1089	534	230	5	12	59	108	213	21	112	25	646	42	832	0.06	3.10	2.00	0.84	0.035
Max	7.53	11,560	5664	1053	42	133	1816	189	3408	47	1920	45	2716	170	10,094	0.22	13.80	3.10	0.98	0.068
Mean	7.17	4205	2061	398	17	41	537	150	1262	35	462	33	1162	78	3262	0.13	6.04	2.55	0.91	0.052
SD	0.20	3442	1687	211	9	30	659	26	1230	8	519	7	544	42	2997	0.05	3.43	0.29	0.04	0.011

Min minimum, *Max* maximum, *SD* standard deviation
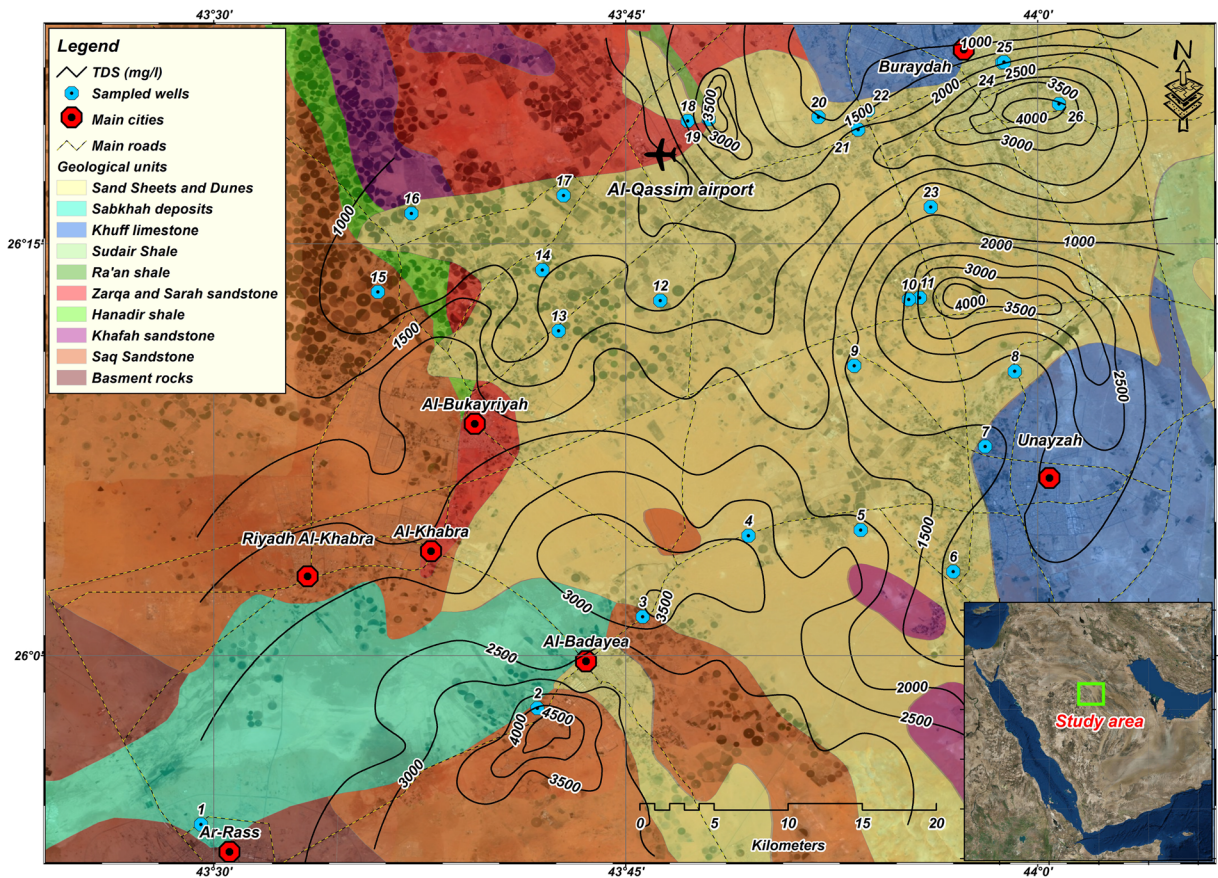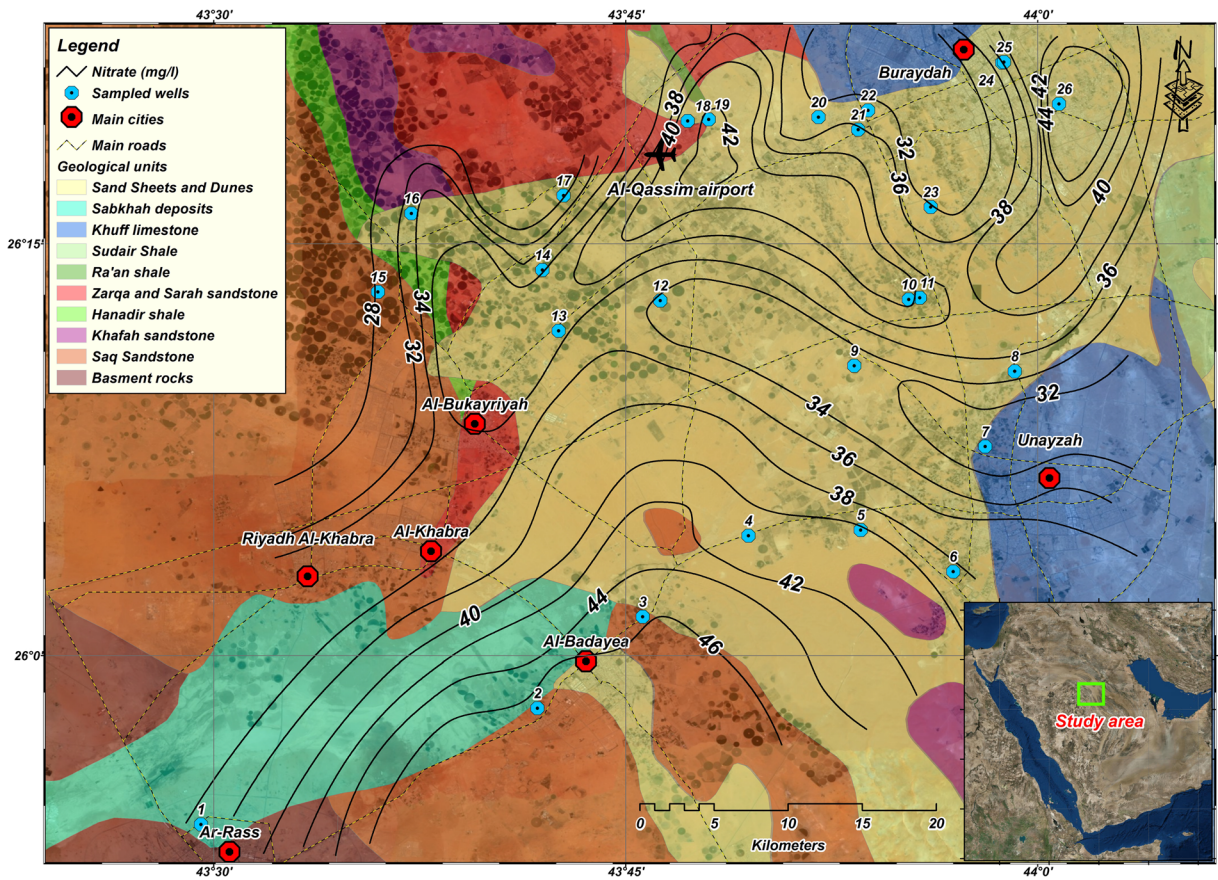
Fig. 3 Spatial distribution of groundwater salinity of Saq Aquifer

The HCO₃⁻ ion concentration extended between 108 and 189 mg/L, with an average value of 150 mg/L.

The salinity varied from the Saq outcrop areas to the confined parts depending on the geologic and hydrogeological situations. Generally, the Saq groundwater salinity showed an increasing trend in the outcrop area in the western part and decreased in the confined area to the east. Deviations in the general salinity trends were the result of several conditions: (i) modern groundwater recharge with relatively brackish water, especially in sabkha depression areas in the west, where runoff water percolates to reach the groundwater after intensive evaporation (Fig. 3); (ii) irrigation return flow in the dense agricultural areas in the south and northwest (Fig. 3); and (iii) overexploitation and draining of the deep relatively saline zones of the aquifer, where salinity differs greatly in several adjacent wells, especially in the dense urbanized areas of Al-Badayea, Al-Khabra, Riyadh Al-Khabra, Al-Bukayriyah, Unayza, and Buraydah (Fig. 3).

The sampled groundwater nitrate concentrations extended between 21 and 47 mg/L, with an average value of 35 mg/L and standard deviation of 8. The spatial distribution of the nitrate concentrations plotted by means of the fitted semi-variogram model shows high peaks in the dense urbanized and agricultural areas (Fig. 4). Generally, NO_3^- in natural groundwater might fluctuate up to 10 mg/L; however, anthropogenic activities like agriculture, septic systems, and animal manure can increase the concentration to rise above the WHO permissible limit of 50 mg/L (Widory et al. 2004; USEPA 2012). In the Al-Badayea, Al-Khabra, and Buraydah urban areas, the sewer systems are not advanced and overflowing cesspit are used, resulting in high peak NO_3^- concentrations. Additionally, high concentrations are detected in the southern and western parts, where without the confining bed of the Hanader shale, anthropogenic pollutants like fertilizers and nutrients can leach through the surface to reach the groundwater.

Fig. 4 Spatial distribution of the nitrate concentrations in the groundwater of Saq Aquifer

Although phosphate is highly immobile in soils because it is adsorbed by soil colloids or organic matter, high concentrations were observed in the groundwater samples. The maximum allowable level of HPO_4^{2-} in drinking water must not exceed 0.025 mg/L according to the United States Environmental Protection Agency (USEPA) (EPA 1993). The concentrations in all the water samples exceeded this limit, varying from 0.035 to 0.068 mg/L. The Swaziland Water Service Corporation (2010) and the European Commission have proposed a higher threshold for HPO_4^{2} (< 1 and 0.5 mg/L, respectively), and the concentrations of all the analyzed water samples lay within this higher tolerance. The high concentrations of HPO_4^{2-} might be attributed to inadequate management of fertilization and the leaching of nutrients and detergents. Another factor responsible for the greater HPO_4^{2-} concentrations in the groundwater could be the practice of large amounts of phosphate fertilizer in areas where the irrigation efficiency of the sandy soils are low.
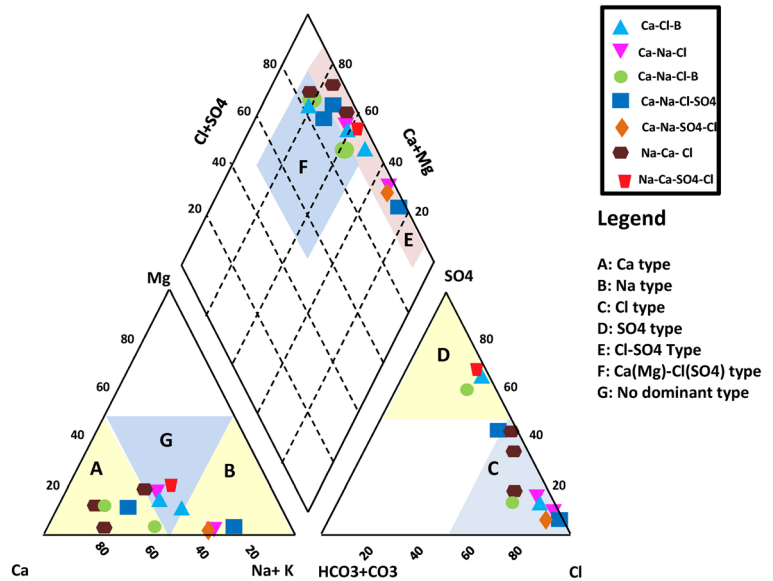
Water types and facies

Seven different groundwater types were identified in the study area (Table 2). The hydrochemical data were plotted in a Piper diagram (Fig. 5), which provided a

Table 2 Distribution of water type for the 26 groundwater samples from Saq Aquifer

| Type	Water composition	Number of samples	Percentage of samples
I	Ca–Cl–HCO$_3$	7	26.9
II	Ca–Na–Cl	4	15.4
III	Ca–Na–Cl–HCO$_3$	3	11.5
IV	Ca–Na–Cl–SO$_4$	3	11.5
V	Ca–Na–SO$_4$–Cl	2	7.7
VI	Na–Ca–Cl	6	23.1
VII	Na–Ca–SO$_4$–Cl	1	3.9

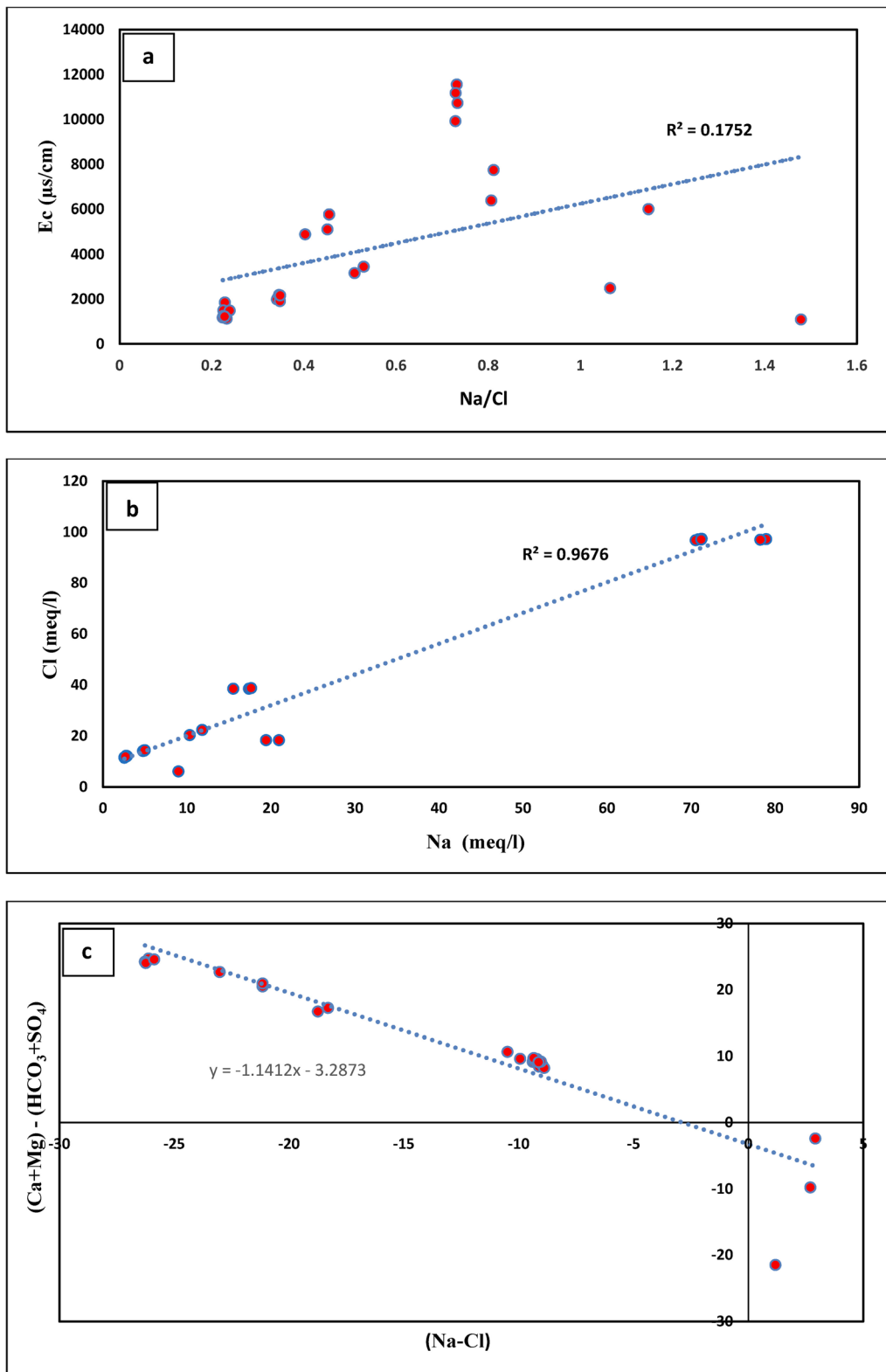**Fig. 5** Piper diagram for the groundwater samples

good method to classify and differentiate the groundwater types (Piper 1944; Aly and Benaabidate 2010; Semerjian 2011).

The majority of the samples were within the Cl–SO$_4$ type of groundwater facies representing alkaline water with prevalent sulfate–chloride ions. Fewer samples were within the Ca(Mg)–Cl(SO$_4$) facies which is characterized by the earth alkaline water with increased alkalis and prevalent sulfate and chloride. The identified facies showed that the samples in general are dominated by the presence of Ca^{2+} and Cl$^-$ ions. The Na–Ca–Cl and Ca–Na–Cl facies represent groundwater influenced by rock–water interaction (halite dissolution and ion exchange). The Ca–Na–Cl–HCO$_3$ and Ca–Na–Cl–SO$_4$ facies represent reverse ion exchange and presence of some shale intercalations. The Ca–Na–SO$_4$–Cl water type is influenced by reverse ion exchange, whereas the Na–Ca–SO$_4$–Cl type represents ion exchange.
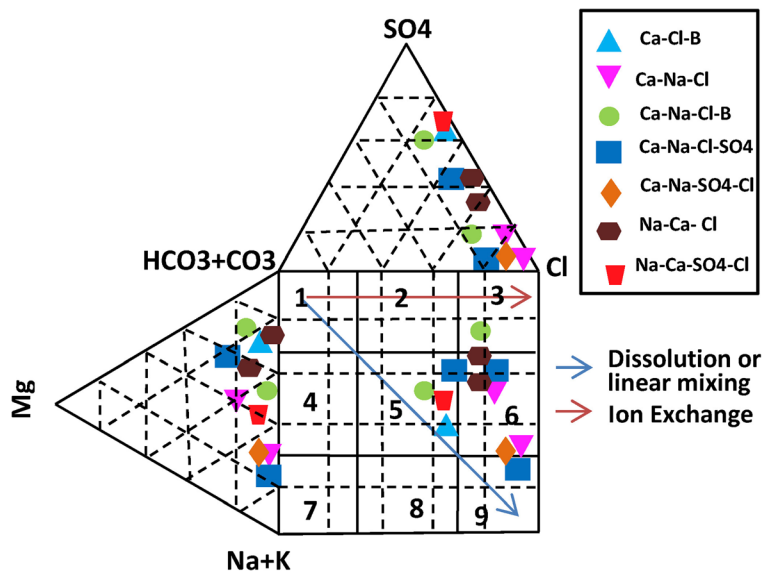
Fig. 6 Durov diagram of the groundwater samples from Saq Aquifer

Fig. 7 Three plots of the Saq groundwater samples. **a** EC versus Na^+/Cl^- **b** Cl^- versus Na^+ **c** $(Ca^{2+} + Mg^{2+})–(HCO_3^- + SO_4^{2-})$ versus $Na^+–Cl^-$
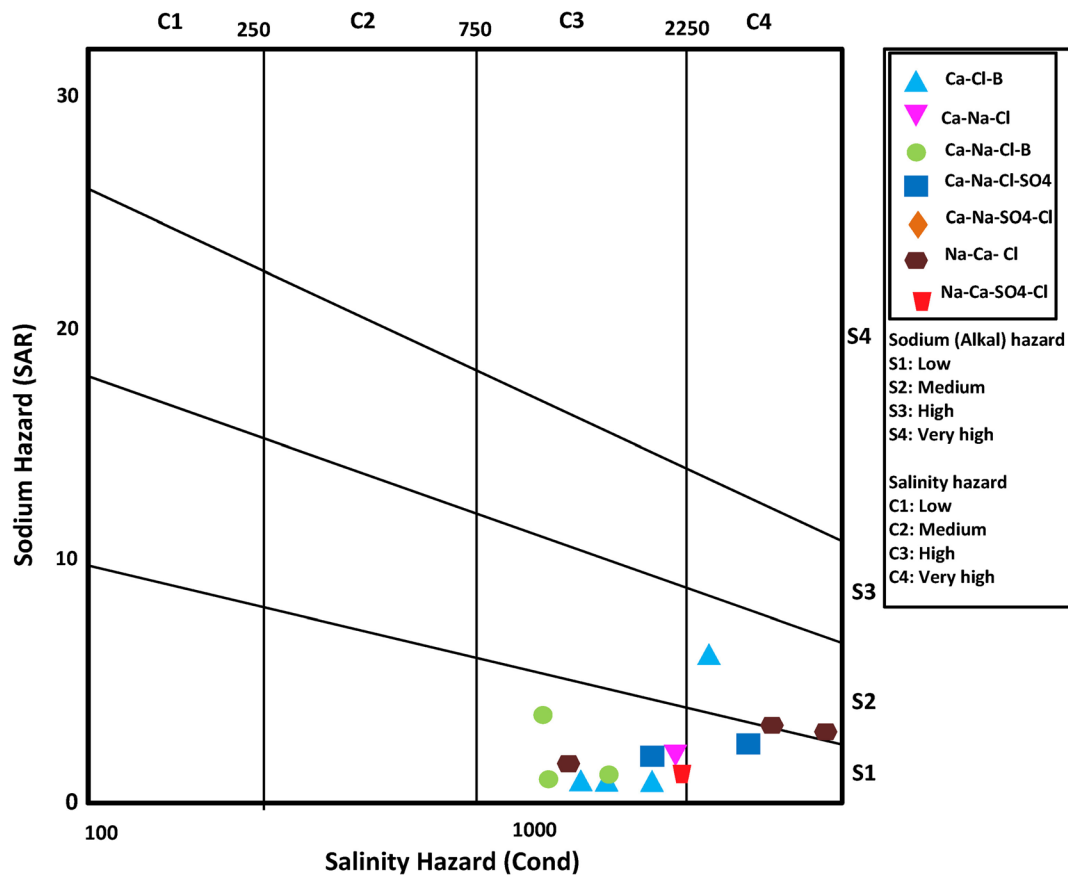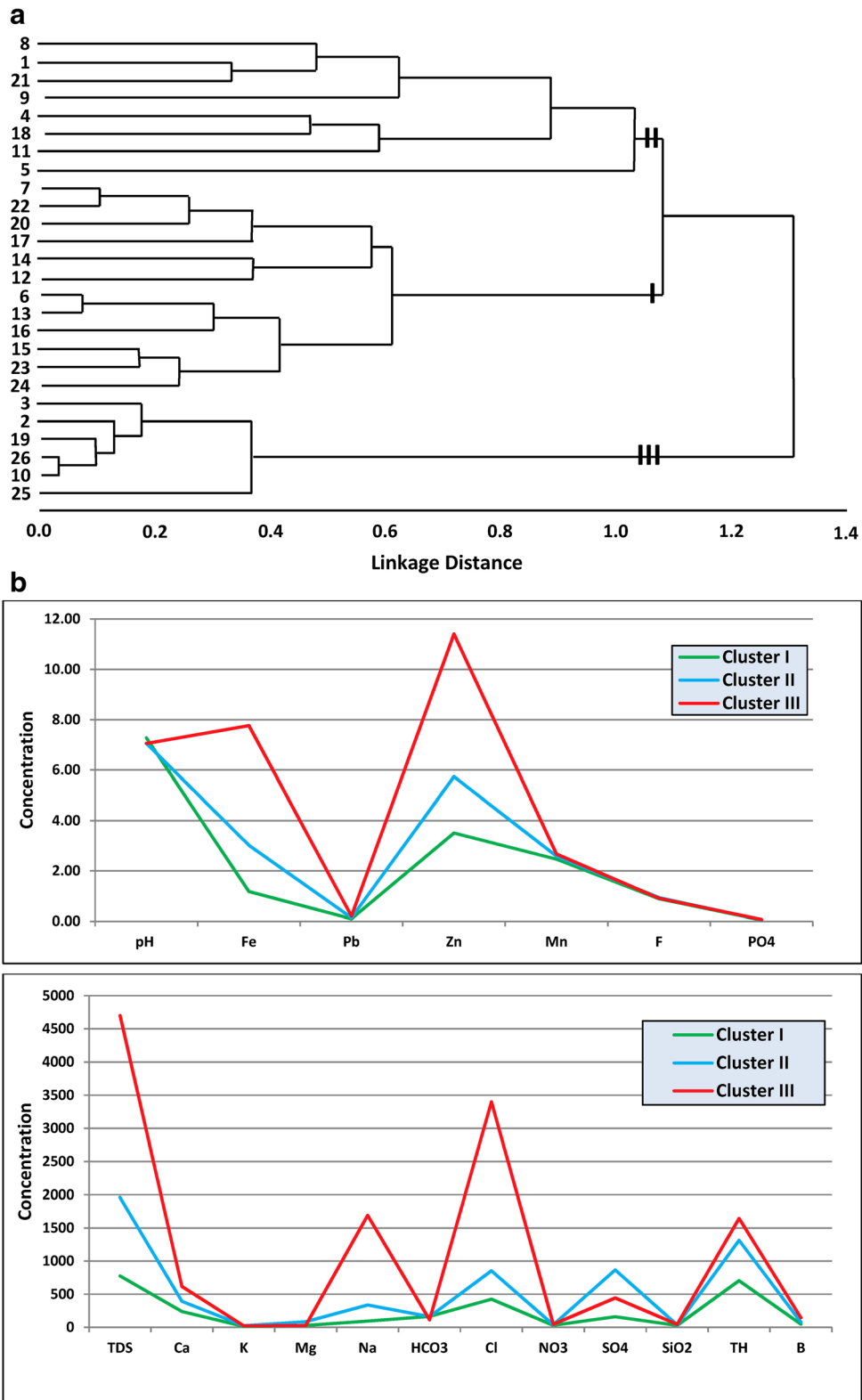
**Fig. 8** SAR diagram of the groundwater samples

The hydrochemical processes affecting groundwater that indicate the original genesis can be best explained with the Durov diagram (Lloyd and Heathcote 1985). The groundwater samples fell into the 3, 5, 6, and 9 fields of the Durov plot (Fig. 6). The Durov plot of the groundwater samples indicated that most of the samples are in the phase of mixing and dissolution, with few samples experiencing reverse ion exchange. However, most of groundwater samples fell into field 6, which represents the mixed type of groundwater facies and indicates the reverse ion exchange process, since the chloride and sodium ions are dominant. Field 9 characterizes simple halite dissolution reflecting the continuity of dissolution and the ion exchange process until the end point water of sodium chloride. In field 3, Ca^{2+} and SO_4^{2-} are dominant representing simple dolomite dissolution. Field 5 suggests the mixed type of groundwater facies with no dominant ions.

The EC versus Na/Cl plot was established to investigate the influence of evaporation processes on groundwater chemistry (Jankowski and Acworth 1997). The water samples showed a nonlinear relationship with a correlation coefficient of 0.17, representing that evaporation is not a major process governing the groundwater chemistry in the study area (Fig. 7a). Figure 7b shows a 1:1 equivalent between the Cl^- versus Na^+ concentrations indicating halite dissolution. There are three water sample groups identified in Fig. 7. The first group contains most of the samples and plots along the halite dissolution line (Fig. 7b). The second group is represented by samples with higher values of Cl^- than Na^+. The excess of Cl^- in this water group might be due to the removal of Na^+ from the groundwater system by reverse ion exchange or the addition of Cl^- from anthropogenic sources. The third group is characterized by samples with higher concentrations of Na^+ than Cl^-, which might be attributed to silicate weathering or ion exchange reactions. The ion exchange reaction hypothesis was tested by plotting Na^+–Cl^- versus (Ca^{2+} + Mg^{2+})–(HCO_3^- + SO_4^{2-}) as shown in Fig. 7c. Base

Fig. 9 a Q-mode dendrogram using the weighted pair-group average and the 1-Pearson *R* values for the groundwater samples. **b** Average variable values for the different clusters
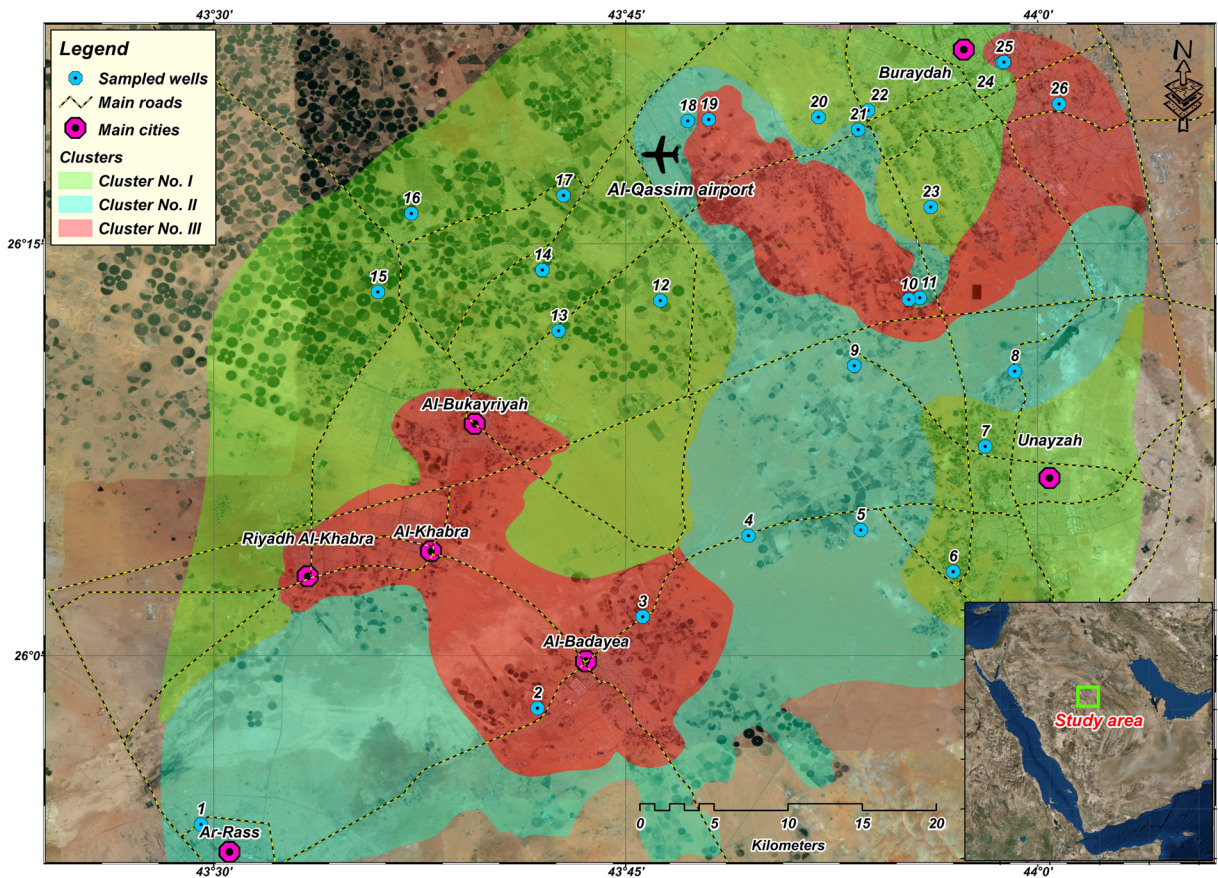
Fig. 10 Spatial distribution of the Q-mode dendrogram groundwater clusters

ion exchange reactions within the groundwater should exhibit a slope of − 1.0, with the trend line intercept close to 0 on the y-axis (Fisher and Mullican 1997; Rajmohan and Elango 2004). The groundwater samples plotted with a slope value of − 0.97 and an intercept of − 0.3, which showed that the Ca^{2+}, Mg^{2+}, and Na^+ concentrations are consistent through the ion exchange process.

The saturation indices of anhydrite, gypsum, halite, calcite, and quartz phase minerals were calculated for the groundwater samples by means of the PHREEQC computer package (Parkurst and Appelo 2011). The results showed that all samples were undersaturated in regard to anhydrite, gypsum, and halite, indicating the possibility for further leaching the salts and dissolution of these minerals when encountered in the aquifer media. The saturation indices for quartz were supersaturated, while nearly 46% of the samples were in equilibrium or slightly saturated with respect to calcite.

The geospatial distributions, classifications, and plotting diagrams showed that the main prevailing process is the simple dissolution of evaporites with mixing from irrigation return flow. Intensive evaporation influenced by low rainfall concentrates the salts in the soil forming sabkhas in the outlet depressions of the wadi, which can be later leached by consequent runoff water. The groundwater quality in this area has deteriorated due to extensive exploitation in the dense urban and farming areas.

Assessment of groundwater quality

According to WHO standards, the pH values of the water samples are in the range of permissible drinking water limits (WHO 2011). Meanwhile, all the water samples surpassed the Ca^{2+} permissible limit (75 mg/L). Nearly 53% of the water samples had Na^+ values that surpassed the WHO permissible limit (200 mg/L). Only 23, 54, and 86% of the Mg^{2+}, SO_4^{2-}, and Cl^- ion

concentrations exceeded the WHO desirable limits (50, 250, and 250 mg/L, respectively). The HCO_3^- and HPO_4^{2-} ion concentrations of the water samples were within the safe standards of the WHO (2011) and Swaziland Water Service Corporation (2010) values. The groundwater samples had high iron concentrations that varied between 0.8 and 10.1 mg/L, with an average value of 3.3 mg/L. Although the WHO has not proposed a health-based guideline value for iron, nearly all the water samples exceeded the limits recommended by the USEPA (2017) of 0.3 mg/L. As iron is one of the eight most abundant elements in the Earth's crust, it can simply pollute groundwater. In Saq Aquifer, the presence of iron can be confirmed by field observations, where layers of ferruginous sandstone form part of Saq Aquifer. The existence of iron in groundwater is strongly affected by oxidation and reduction conditions. However, high concentrations of dissolved ferrous iron can occur in solution at sites for either the reduction of ferric oxyhydroxides or the oxidation of ferrous sulfides. Corrosion of well casings and pipes, and bacterial activity might increase iron concentrations in groundwater. The average concentration of lead, boron, zinc, manganese, and fluoride in the groundwater samples was 0.0001, 0.078, 0.006, 0.003, and 0.9 mg/L which are far below the recommended limits by the WHO (2011) for drinking water (0.001, 0.5, 2.0, 0.4, and 1.5 mg/L, respectively).

Plotting the sodium adsorption ratio (SAR) versus the EC can conclude the suitability of the groundwater for agriculture (Fig. 8); however, sodium readily substitutes other cations present in the soil, causing a sodium hazard. The average EC value of the groundwater samples was 4205 μS/cm which is within the very high salinity hazard range. The EC of the groundwater samples fall into three classes, namely, of permissible, permissible to doubtful, and unsuitable for irrigation water. Leaching of the soil is needed in the permissible class, while for the other two classes, good drainage must be practiced. The concentrations of boron, fluoride, manganese, lead, zinc, and iron were far below the recommended permissible limits of trace elements for irrigation water proposed by Rowe and Abdel-Magid (1995).

Multivariate analyses

The cluster analysis was interpreted at the similarity level of 1.25, whereby the water samples were grouped

Table 3 Factor analysis loadings and eigenvalues of the groundwater samples

	Factor 1	Factor 2	Factor 3
pH	− 0.33	− 0.17	− 0.09
EC	0.98	0.08	0.10
TDS	0.98	0.08	0.10
Ca^{2+}	0.77	0.25	0.20
K^+	0.36	− 0.03	0.86
Mg^{2+}	− 0.06	0.55	0.65
Na^+	0.95	0.02	− 0.15
HCO_3^-	− 0.78	− 0.15	0.52
Cl^-	0.97	− 0.07	− 0.05
NO_3^-	0.79	0.42	0.07
SO_4^{2-}	0.15	0.90	− 0.01
SiO_2	0.92	0.23	0.15
TH	0.73	0.36	0.35
B^{3+}	0.98	0.05	0.08
$Fe_{(tot)}$	0.95	0.02	0.08
Pb^{2+}	0.95	0.11	0.19
Zn^{2+}	0.98	0.04	0.07
Mn^{2+}	0.25	0.39	− 0.10
F^-	0.06	0.82	0.06
HPO_4^{2-}	0.85	0.32	0.31
Expl.Var	11.75	2.55	1.84
Prp.Totl	0.59	0.13	0.09
Eigenvalue	12.32	2.37	1.45
Cumulative total variance (%)	61.62	73.45	80.71

into three main clusters (Fig. 9a). The differences between the clusters were determined using the average chemical analysis data and physico-chemical factors. The spatial distribution of the clusters was justified and validated using the salinity and nitrate spatial distributions, land-use influences, and mineral phase equilibria. Cluster I had 12 samples and originated in the northern and southeastern parts of the study area (Fig. 10). This cluster had the lowest TDS values and other ion concentrations with the exception of HCO_3^- (Fig. 9b). These attributes characterize the fresh groundwater zone; however, the aquifer was recharged with meteoric water during the humid Pleistocene and therefore the cluster has slightly higher average pH and HCO_3^- values than the other clusters. Cluster II had eight water samples and extended from the southwestern to northeastern parts of the area. Except for high concentrations of SO_4^{2-}, Mg^{2+}, K^+, and F^-, this cluster
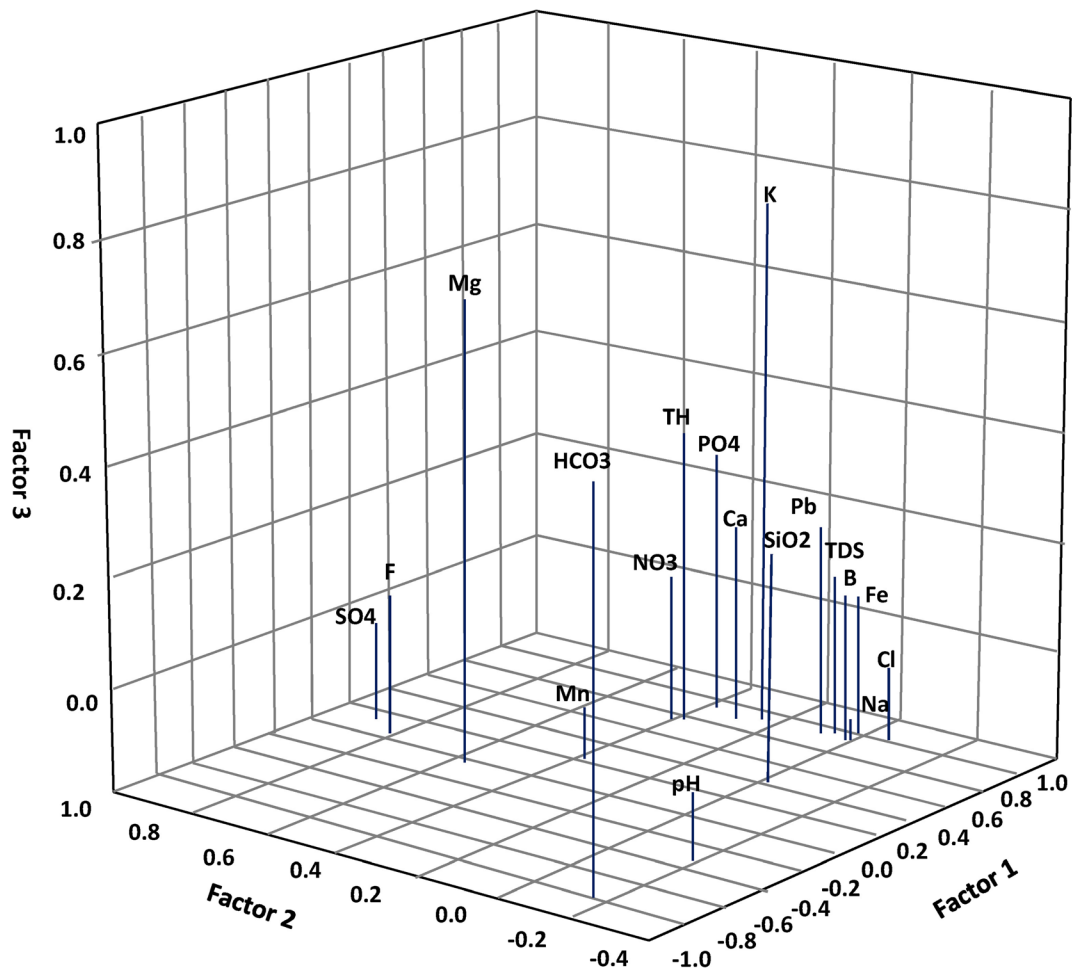
Fig. 11 3-D representation of the loadings for factors 1, 2, and 3 after varimax rotation

had moderate other ion concentration values. This cluster represents the modern groundwater recharge with rainfall and runoff water region where the groundwater flow and vertical percolation are moderate. The water in this cluster has a greater ability to dissolve the different mineral phases found in the aquifer media (calcite, aragonite, gypsum, anhydrite, halite, and fluorite).

The third cluster contained the remainder of the water samples and was initiated in the southwestern and northeastern parts of the study area. This cluster represents the anthropogenic influences, where overexploitation zones of the aquifer are found, water levels are highly declined, and the wells discharge higher salinity water from the deeper zones of the aquifer. These areas are restricted to the dense urban and farming areas in Al-Badayea, Al-Khabra, Riyadh Al-Khabra, Al-Bukayriyah and Buraydah. In these areas, high

concentrations of nitrate are observed, confirming the human impact of dense urbanization and agricultural activities.

The factor analysis showed that there are three main factors affecting groundwater hydrochemistry with a total variance of 80.71% and the smallest eigenvalue of 1.45 (Table 3). The outcome of the factor analysis accounted factor 1 for 61.62 of the total variance and 12.32 of the eigenvalue. Factor 1 had four main processes that resulted in an increase of the water salinity (Table 3 and Fig. 11). These processes included the following: (i) strong positive loadings with respect to the EC, TDS, Cl^-, and Na^+ values indicating the leaching of halite minerals; (ii) high loading of the EC and TDS values with NO_3^- and HPO_4^{2-} indicating a human impact, where the groundwater was influenced by dense urbanization and agricultural activities; (iii)

high loading of Ca^{2+}, and HCO_3^- indicating the dissolution of calcite mineral phases; and (iv) high loading of the EC and TDS values with respect to B^{3+}, $Fe_{(tot)}$, Pb^{2+}, Zn^{2+}, SiO_2, which confirms the dissolution of some of the silicate minerals encountered in the aquifer media. The second factor contained 12.32% of the total variance and 2.37 of the eigenvalue.

This factor has high loadings of SO_4^{2-}, F^-, Mg^{2+}, and NO_3^- and moderate loading with Ca^{2+}, it reflects the dissolution of evaporites which have gypsum and magnesium sulphate mineral phases ($CaSO_4 \cdot 2H_2O$, $MgSO_4 \cdot 7H_2O$), also it shows the human impact of using nitrate and sulphate fertilizers. The high loading of fluoride may be derived from the dissolution of silicate minerals. The third factor accounted for 7.26% of the total variance and 1.84 of the eigenvalue. It had high loadings with respect to K^+, Mg^{2+}, and HCO_3^-, and low loading of Ca^{2+}, which may be attributed to an ion exchange process occurring between K^+ and Mg^{2+} ions that were released in the water by the dissolution of carbonate minerals; however, the water is nearly saturated or oversaturated with respect to the calcite mineral phase.

Conclusions

In arid areas, groundwater is a valuable and vulnerable resource, where rainfall is rare and the recharge rate is low. Due to the aquifer exploitation, declines in groundwater levels have developed and groundwater quality has degraded. The geochemistry of the groundwater of Saq Aquifer was investigated, and the occurrence, relations, and spatial distributions were interpreted. Seven different groundwater types were identified. The majority of the samples were within the Cl–SO_4 type groundwater facies representative of alkaline water. Natural and anthropogenic factors were determined as controls of the groundwater hydrochemistry. The geogenic factors included the dissolution and precipitation of various minerals and ion and reverse ion exchange processes. Most of the groundwater samples, however, were determined as mixed type groundwater facies resulting from reverse ion exchange processes. A smaller number of samples showed simple halite dissolution representative of the continuity of dissolution and ion exchange process until the end point of water. The EC versus Na^+/Cl^- plot showed a nonlinear relationship indicating that

evaporation is not a major process governing the groundwater chemistry. The Cl^- versus Na^+ plot indicates halite dissolution, reverse ion exchange, silicate weathering, and ion exchange reactions. Base ion exchange reactions plot showed that some samples had the Ca^{2+}, Mg^{2+}, and Na^+ concentrations that were interrelated through the ion exchange process. The geochemical equilibrium showed that all samples were undersaturated with respect to anhydrite, gypsum, and halite, indicating the possibility for further leaching and dissolution of minerals encountered in the aquifer media. The human influences affecting the groundwater are aquifer overexploitation, land-use/land-cover change, irrigation return flow, unwise use of fertilizers on farming lands, and wastewater disposal. The groundwater salinity showed a general increasing trend in the outcrop area and decreased in the confined areas. This trend was highly altered by three main factors: modern groundwater recharge with relatively brackish water, irrigation return flow in the dense agricultural areas in the south and northwest, and the overexploitation and draining of the deep relatively saline zones of the aquifer. The spatial distribution of nitrate showed high peaks in the dense urbanized and agricultural areas; however, the sewer systems are not adequate and overflowing cesspits are used. High concentrations of nitrate and phosphates were observed in the southern and western parts of the area, where the confining bed of Hanader shale is absent and therefore, anthropogenic pollutants like fertilizers and nutrients can leach through the surface reaching the groundwater. In the confined areas, nearly all of the groundwater samples were deemed suitable for drinking and irrigation purposes, while in the outcrop area and dense urbanized and irrigated locations, some limitations were found due to factors affecting the groundwater salinity and nitrate concentrations. The cluster analysis interpreted the data into three main clusters. Cluster I characterized the fresh groundwater zone; however, the aquifer was recharged with meteoric water during the humid Pleistocene. Cluster II represented modern groundwater recharge by rainfall and runoff water. Cluster III represented anthropogenic influences and identified the higher human impact overexploitation zones. The factor analysis showed that there were three main factors affected the groundwater hydrochemistry. The first factor had four main influences resulting in increasing the salinity, namely, the leaching of halite minerals, human impacts where groundwater is contaminated by dense urbanization

and agricultural activities, the dissolution of calcite mineral phases, and some silicate minerals. The second factor represented the dissolution of evaporites and also indicated the use of nitrate and sulfate fertilizers. The third factor may be attributed to ion exchange between K^+ and Mg^{2+} ions, which are released by carbonate mineral phases. The integration of the geospatial distributions, classifications, and multivariate analyses showed that the main dominant processes affecting the hydrochemistry and groundwater quality was the simple dissolution of evaporates with mixing from irrigation return flow. The intensive evaporation affected by low rainfall concentrates the salts in the soil forming sabkhas. The groundwater quality in dense urban and agricultural areas has deteriorated due to extensive exploitation. This study shows that groundwater in arid areas is highly vulnerable; therefore, integrated management of water resources and uses founded on knowledge-based planning and allocation of water use is critical.

References

Ahmed, I., Nazzal, Y., Zaidi, F., Al-Arifi, N., Ghrefat, H., & Naeem, M. (2015). Hydrogeological vulnerability and pollution risk mapping of the Saq and overlying aquifers using the DRASTIC model and GIS techniques, NW Saudi Arabia. *Environmental Earth Science, 74*(2), 1303–1318.

Al-Bassam, A. (2006). Evaluation of ground water quality in the Al-Qassim area, Saudi Arabia, using cluster and factor analyses. *Kuwait Journal of Science, 33*(2), 101–121.

Almazroui, M. (2011). Calibration of TRMM rainfall climatology over Saudi Arabia during 1998– 2009. *Atmospheric Research, 99*, 400–414.

Aly, A., & Benaabidate, L. (2010). Salinity of water resources in the Siwa Oasis: monitoring and diagnosis. In T. A. Brikle (Ed.), *Water-rock interaction*. London: Taylor & Francis Group.

APHA (1995). Standard methods for the examination of water and wastewater. American public Health association, 19th edition, Washington DC. p 45.

Burdon, D. J. (1982). Hydrogeological conditions in the Middle East. *Quarterly Journal of Engineering Geology and Hydrogeology, 15*, 71–82.

Bureau de Récherches Géologigues et Miniéres (BRGM) (1985). Water, agriculture, and soil studies of Saq and overlying aquifer, 6 vols, Rep. Min. Agri. Water, Saudi Arabia.

Bureau de Récherches Géologigues et Miniéres (BRGM) (2006). Investigations for updating the groundwater mathematical model(s) of the Saq and overlying aquifers. Ministry of Water and Electricity – Kingdom of Saudi Arabia.

Chaudhuri, S., & Ale, S. (2014). An appraisal of groundwater quality in Seymour and Blaine aquifers in a major agro-ecological region in Texas, USA. *Environmental Earth Science, 71*(6), 2765–2777.

Cloutier, V., Lefebvre, R., Therrien, R., & Savard, M. (2008). Multivariate statistical analysis of geochemical data as indicative of the hydrogeochemical evolution of groundwater in a sedimentary rock aquifer system. *Hydrogeology Journal, 353*, 294–313.

Davis, JC. (2002). Statistics and data analysis in geology, 3rd Ed. Wiley, New York ISBN-9780471172758.

El Alfy, M. (2004). Geochemical characteristics and pollution assessment of the groundwater of the Quaternary aquifer, Qatia area, North Sinai, Egypt. 6th Intern. Conf. Geochemistry. Alex. Univ. Egypt. p. 271–292.

El Alfy, M. (2013). Hydrochemical modeling and assessment of groundwater contamination in Northwest Sinai, Egypt. *Water Environment Research, 85*(3), 211–223.

El Alfy, M., & Faraj, T. (2017). Spatial distribution and health risk assessment for groundwater contamination from intensive pesticide use in arid areas. *Environmental Geochemistry and Health, 39*(1), 231–253.

El Alfy, M., & Merkel, B. (2006). Hydrochemical relationships and geochemical modeling of ground water in Al Arish area, North Sinai, Egypt. *American Institute of Hydrology (AIH), Hydrological Science and Technology Journal, 22*(1–4), 47–62.

El Alfy, M., Lashin, A., Al-Arifi, N., & Al-Bassam, A. (2015). Groundwater characteristics and pollution assessment using integrated hydrochemical investigations GIS and multivariate geostatistical techniques in arid areas. *Water Resources Management, 29*, 5593–5612.

El Alfy, M., Lashin, A., Abdalla, F., & Al-Bassam, A. (2017). Assessing the hydrogeochemical processes affecting groundwater pollution in arid areas using an integration of geochemical equilibrium and multivariate statistical techniques. *Environmental Pollution, 229*, 760–770.

Environmental Protection Agency-USA-EPA (1993) National interim primary drinking water regulations, part 141, Fed. Reg. 40(248):59566–59588.

FAO (2009). Groundwater management in Saudi Arabia, draft synthesis report. Food and Agriculture Organization of the United Nations, Rome, p14.

Fisher, R. S., & Mullican, W. F. (1997). Hydrochemical evolution of sodium-sulphate and sodium-chloride groundwater beneath the northern Chihuahuan Desert, Trans-Pecos, Texas, USA. *Hydrogeology Journal, 5*, 4–16.

Furi, W., Razack, M., Abiye, T., Kebede, S., & Legesse, D. (2012). Hydrochemical characterization of complex volcanic aquifer in a continental rifted zone: the Middle Awash basin, Ethiopia. *Hydrogeol Journal, 20*, 385–400.

Gemail, K., El Alfy, M., Ghoneim, M., Shishtawy, A., & Abd El-Bary, M. (2017). Comparison of DRASTIC and DC

resistivity modeling for assessing aquifer vulnerability in the central Nile Delta, Egypt. *Environmental Earth Sciences, 76*(9), 350.

Gleeson, T., Wada, Y., Bierkens, M. F., & van Beek, L. P. (2012). Water balance of global aquifers revealed by groundwater footprint. *Nature, 488*(7410), 197–200.

Hatcher, L., & Stepanski, E. (1994). *A step-by-step approach to using the SAS system for univariate and multivariate statistics*. Cary, NC: SAS Institute Inc..

Jado, AR., Zotl, JG. (1984). Quaternary period in Saudi Arabia, vol. 2. Springer, New York.

Jankowski, J., & Acworth, R. I. (1997). Impact of debris-flow deposits on hydrogeochemical processes and the development of dryland salinity in the Yass River catchment, new South Wales, Australia. *Hydrogeology Journal, 5*(4), 71–88.

Kaiser, H. (1958). The varimax criteria for analytical rotation in factor analysis. *Psychometria, 23*, 187–200.

Kaufman, L., & Rousseuw, P. J. (1990). *Finding groups in data: an introduction to cluster analysis* (p. 344). New York: Wiley.

Lavoie, R., Joerin, F., Vansnick, J. C., & Rodriguez, M. J. (2015). Integrating groundwater into land planning: a risk assessment methodology. *Journal of Environmental Management, 154*, 358–371.

Lloyd, J. W., & Heathcote, J. A. (1985). *Natural inorganic hydrochemistry in relation to groundwater: an introduction* (p. 294). Oxford: Clarendon Press.

Lloyd, J. W., & Pirn, R. H. (1990). The hydrogeology and groundwater resources development of the Cambro-Ordovician sandstone aquifer in Saudi Arabia and Jordan. *Journal of Hydrology, 121*, 1–20.

Lockhart, K., King, M., & Harter, T. (2013). Identifying sources of groundwater nitrate contamination in a large alluvial groundwater basin with highly diversified intensive agricultural production. *Journal of Contaminant Hydrology, 151*, 140–154.

Merkel, B., & Planer-Friedrich, B. (2008). *Groundwater geochemistry, a practical guide to modeling of natural and contaminated aquatic systems* (2nd ed.p. 230). Berlin Heidelberg: Springer-Verlag.

Parizi, H. S., & Samani, N. (2013). Geochemical evolution and quality assessment of water resources in the Sarcheshmeh copper mine area (Iran) using multivariate statistical techniques. *Environmental Earth Sciences, 69*(5), 1699–1718.

Parkurst, D., Appelo, C. (2011) User's guide to PHREEQC (V.2): a computer program for speciation, batch-reaction, one-dimensional transport, and inverse geochemical calculations. U.S. Department of the Interior/U.S. Geological Survey, Washington.

Piper, A. M. (1944). A graphic procedure in the geochemical interpretation of water analysis. *Transactions of the American Geophysical Union, 25*, 914–928.

Powers, R. W., Ramirez, L. F., Redmond, C. D., & Elberg, E. L. (1966). Geology of the Arabian Peninsula. *Geological Survey Professional Paper, 560*, 1–147.

Rajmohan, N., & Elango, L. (2004). Identification and evolution of hydrogeochemical processes in the groundwater environment in an area of the Palar and Cheyyar River Basins, Southern India. *Environ Geology, 46*(1), 47–61.

Rasool, A., Xiao, T., Baig, Z., Masood, S., Mostofa, K., & Iqbal, M. (2015). Co-occurrence of arsenic and fluoride in the groundwater of Punjab, Pakistan: source discrimination and health risk assessment. *Research Journal of Chemical & Environmental Sciences, 22*, 19729–19746.

Rowe, D., & Abdel-Magid, I. (1995). *Handbook of wastewater reclamation and reuse*. Boca Raton: CRC Press, Inc.

Salman, A. S., Zaidi, F. K., & Hussein, M. T. (2014). Evaluation of groundwater quality in northern Saudi Arabia using multivariate analysis and stochastic statistics. *Environmental Earth Science, 74*(12), 7769–7782.

Semerjian, L. A. (2011). Quality assessment of various bottled waters marketed in Lebanon. *Environmental Monitoring and Assessment, 172*, 275–285.

Singh, C. K., & Mukherjee, S. (2015). Aqueous geochemistry of fluoride enriched groundwater in arid part of western India. *Research Journal of Chemical & Environmental Sciences, 22*, 2668–2678.

Tabachnick, B. G., & Fidell, L. (2006). *Using multivariate statistics* (5th ed.). NY: Allyn & Bacon.

USEPA (2012). 2012 edition of the drinking water standards and health advisories, EPA 822-S-12-001, Office of Water, U.S. Environmental Protection Agency: Washington, D.C.

Widory, D., Kloppmann, W., Chery, L., Bonnin, J., Rochdi, H., & Guinamant, J. L. (2004). Nitrate in groundwater: an isotopic multi-tracer approach. *Journal of Contaminant Hydrology, 72*(1), 165–188.

World Bank (2012) Policy options for a national water strategy, Part One: Water Resources Assessment, Challenges and Options. Ministry of water and electricity, Riyadh, Saudi Arabia.

World Health Organization (WHO) (2011) Guidelines for drinking water quality, fourth edition. ISBN: 9789241548151, p 564.

Zaidi, F. K., & Mukhopadhyay, M. (2015). Morphometric analysis of the scoria cones and drainage pattern for the quaternary and older volcanic fields in parts of the Large Igneous Province (LIP), Saudi Arabia. *Journal of African Earth Sciences, 110*, 1–13.